Aeolian Research 20 (2016) 7–23

Contents lists available at ScienceDirect

Aeolian Research

journal homepage: www.elsevier.com/locate/aeolia

Sedimentological and mineralogical characteristics of the Pleistocene loess/paleosol sections in the Eastern Croatia

Lidija Galović *

Croatian Geological Survey, Sachsova 2, 10000 Zagreb, Croatia

ARTICLE INFO

Article history:
Received 31 March 2015
Revised 29 October 2015
Accepted 29 October 2015

Keywords:
Modal analysis
Loess
Paleosol
Laminated sediments
SEM
Pleistocene

ABSTRACT

In the Eastern Croatia impressive loess–paleosol successions up to 30 m thick are exposed. In the Zmajevac I section three paleosols are intercalated in loess while in the Zmajevac, Erdut and Šarengrad sections there are four paleosols are intercalated in loess. IRSL age estimates of 17.8 ± 1.9 and 217 ± 22 ka. In all investigated sections, alluvial sediments are intercalated in the loess deposits, indicating periods of fluvial activity.

Strongly abraded typical aeolian spherical grains characterized by pitted well-rounded surface that was developed during transportation have original crystal surface almost destroyed. Surface of quartz grains preserves micro textures characteristic for all transport medias that it has been exposed to. However, muscovite grain surface enable successful distinguishing if the last transport was by wind or by aquatic media. Characteristic of all horizons with muscovite as a dominant mineral is recent settling of organisms. Beside the Danube, Drava and Sava River flood plains, part of the analyzed sediments also originates from regional Tertiary sediments which are rich in granite (as a muscovite-bearing rock), indicating the local influence. Enrichment of pyroxenes in the Šarengrad section points to the Dinaride Ophiolite Zone as its source of origin eroded by the Sava River southern tributaries. Šarengrad section is the southernmost among the analyzed sections and the southern edge of the Carpathian Basin. Thus, beside the Alpine region, the mineral composition is influenced by minerals from the Dinaride Ophiolite Zone in Bosnia. Warming periods are not represented just by paleosols, but also with laminated alluvial sediments.

1. Introduction

In Croatia, Quaternary alluvial, marshy and lake sediments are widespread in Eastern Croatia (Figs. 1 and 2). They are mostly overlain by aeolian-derived sediments, e.g. loess, that were formed during the cold periods of the Pleistocene. The loess deposits are mainly situated in the eastern part of the country, where they reach the thickness up to 40 m.

In the study area, two main processes cause exposures of loess sections, namely (neo) tectonically uplifted area of the Bansko Brdo (Pamić and Pikija, 1987) and the loess sediments exposed by lateral river erosion, the latter forming steep cliffs along the Danube River. These loess successions are excellent archives of climate change, including environmental changes during the Middle and Late Pleistocene time periods (Galović et al., 2009, 2011; Marković et al., 2009, 2011; Újvári et al., 2014). According to Bronger (1976, 2003), at least six paleosols are intercalated in the loess sections from Eastern Croatia, covering the time period of the Middle and Late Pleistocene (Galović et al., 2009). The famous loess sections from Vukovar, near St. Filip and Jacob's church, are situated on the west bank of the Danube River and have been extensively investigated for about 100 years by means of mineralogical, paleontological, chronological, geomorphological, pedological and climatological studies (Bronger, 1976, 2003; Galović and Mutić, 1984; Gorjanović-Kramberger, 1912, 1914; Mutić, 1990; Poje, 1985, 1986; Rukavina, 1983; Singhvi et al., 1989; Wacha and Frechen, 2011). After the first luminescence dating approach to the sections investigated in this study (Galović et al., 2009), specific investigations were carried out for the Zmajevac loess–paleosol sequences (Banak et al., 2012, 2013; Galović, 2014; Molnár et al., 2010) and the Šarengrad sequence (Galović 2014; Galović et al., 2011; Hupuczi et al., 2010; Wacha et al., 2013).

These sequences provide very detailed records of climate change correlating to MIS 2-8, especially if compared with other sections in the Carpathian Basin (Antoine et al., 2009; Bokhorst et al., 2009; Buggle et al., 2008, 2011; Fitzsimmons et al., 2012; Frechen and Pécsi, 2004; Haase et al., 2007; Marković et al., 2009, 2011, 2012; Singhvi et al., 1989; Újvári et al., 2014).

* Tel.: +385 1 61 60 779, mob: +385 99 310 78 02; fax: +385 1 61 44 718.
E-mail address: lidija.galovic@hgi-cgs.hr

http://dx.doi.org/10.1016/j.aeolia.2015.10.007
1875-9637/© 2015 Published by Elsevier B.V.

The scope of this work is to investigate the modal composition and to compare it with geochemical, geochronological and sedimentological data of analyzed loess/paleosol sediment successions. Sedimentological data (grain-size coefficients), geochemical content of major, trace and rare earth elements (REE) and acidity (pH) (Galović, 2014; Galović et al., 2009, 2011; Wacha et al., 2013) accompanied with previously published data on IRSL dating, grain-size distribution, organic carbon content (TOC) and $CaCO_3$ content (Galović et al., 2009), highlighted the main characteristics of paleosols and the degree of their pedogenesis. Based on these results, another aim of modal analyses (mineral composition of heavy and light mineral fraction) was to define the source area of sediments that served as the parent material of analyzed sediments. Detailed research of the mineralogical composition of Quaternary sediments developed in the Pannonian and Adriatic regions showed their polygenetic origin (Durn, 2003; Durn et al., 1999, 2007, 2014; Rubinić et al., 2014, 2015). The present contribution focused on assessment of the specific heavy and light mineral composition as fingerprint of the sediment that was the parent material of analyzed soils/paleosols.

Furthermore, in each investigated succession, beside loess-derivated sediments, there are a few meters of intercalated laminated alluvial sediment composed of loess-derivated material eroded from its drainage basin. Such an ordinarily appearance of laminated sediment in loess successions is typical for marginal conditions on south edge of the Carpathian basin. Since the only difference between samples from laminated horizons and the rest of sampled horizons is the last media (mechanism) of transport

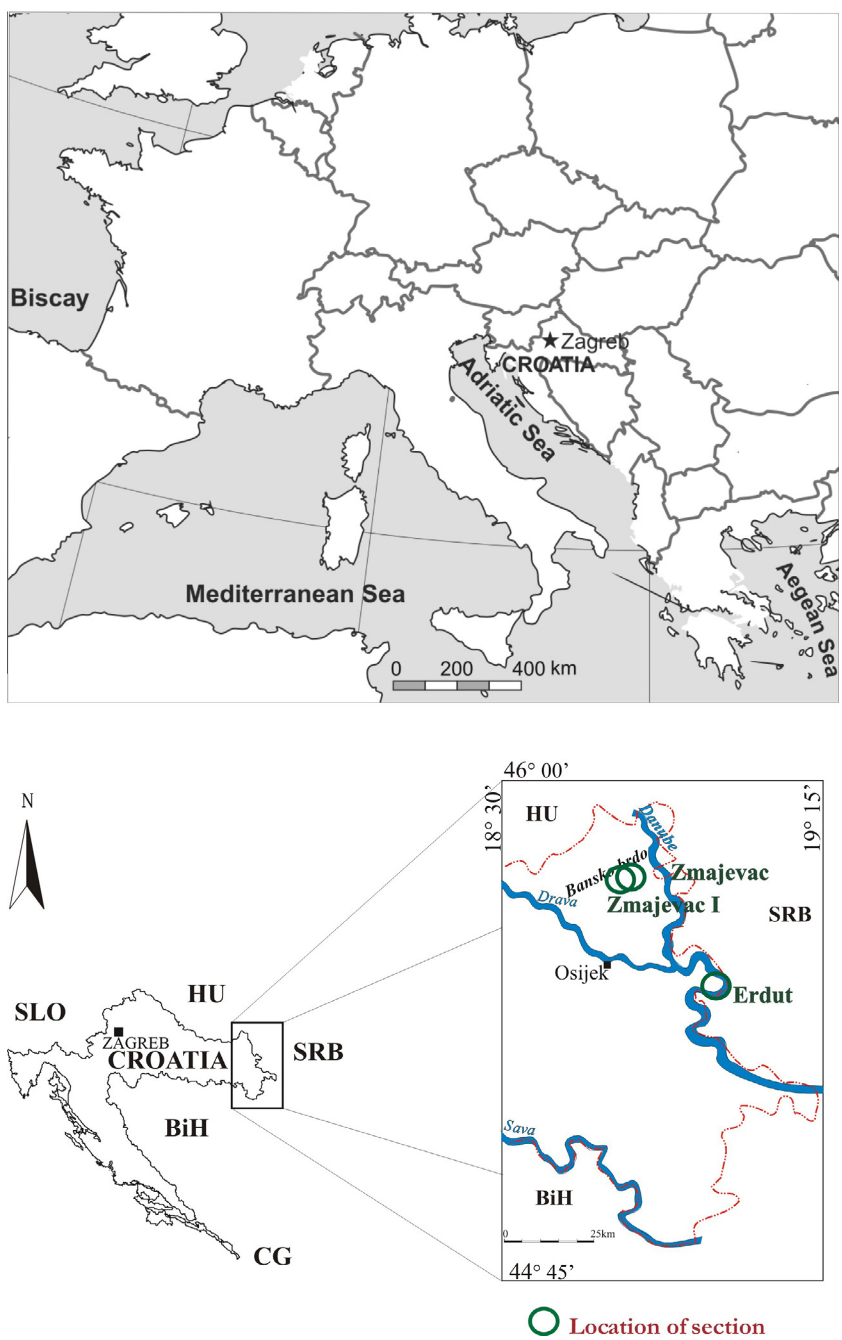

Fig. 1. Map showing the position of the sections under the investigation in the Eastern Croatia.

(water or wind), another scope of this work was to establish differences in shape and habitus of monomineral grains that was exposed to water or wind as the last transporter.

2. Geological setting

During the Pleistocene, aeolian sediments were deposited in lakes, pools and shallow marshes in the Croatian lowland (Bačani et al., 1999) (Fig. 2). Part of these sediments were eroded by the Danube, Drava and Sava Rivers and/or re-deposited downstream as alluvial sediments. Similar deposits were reported and investigated from the Abony section in Hungary (Frechen and Pécsi, 2004).

Detailed lithostratigraphical subdivisions of the four investigated sections from the three localities (Zmajevac, Zmajevac I, Erdut and Šarengrad) are represented in previous works by Galović et al. (2009, 2011) and Galović (2014).

2.1. Zmajevac

The Bansko Brdo is an asymmetric tectonic structure (horst) elongated NE–SW with elevation of about 243 m above sea level (asl.) which is the highest in the study area. Tectonic activity caused synsedimentary effusion of basaltic andesite and deposition of volcanic breccias. The Miocene age of andesites is confirmed by K–Ar dating (14.5 ± 0.4 and 13.8 ± 0.4 Ma) at two locations (Pamić and Pikija, 1987). Loess is exposed on top of the volcano-clastic material. More recent, tectonic uplift formed a complex horst – the Bansko Brdo. Loess–paleosol sequences are exposed along its south-eastern slope. These neotectonic movements are still active (Galović et al., 2009) (Fig. 2).

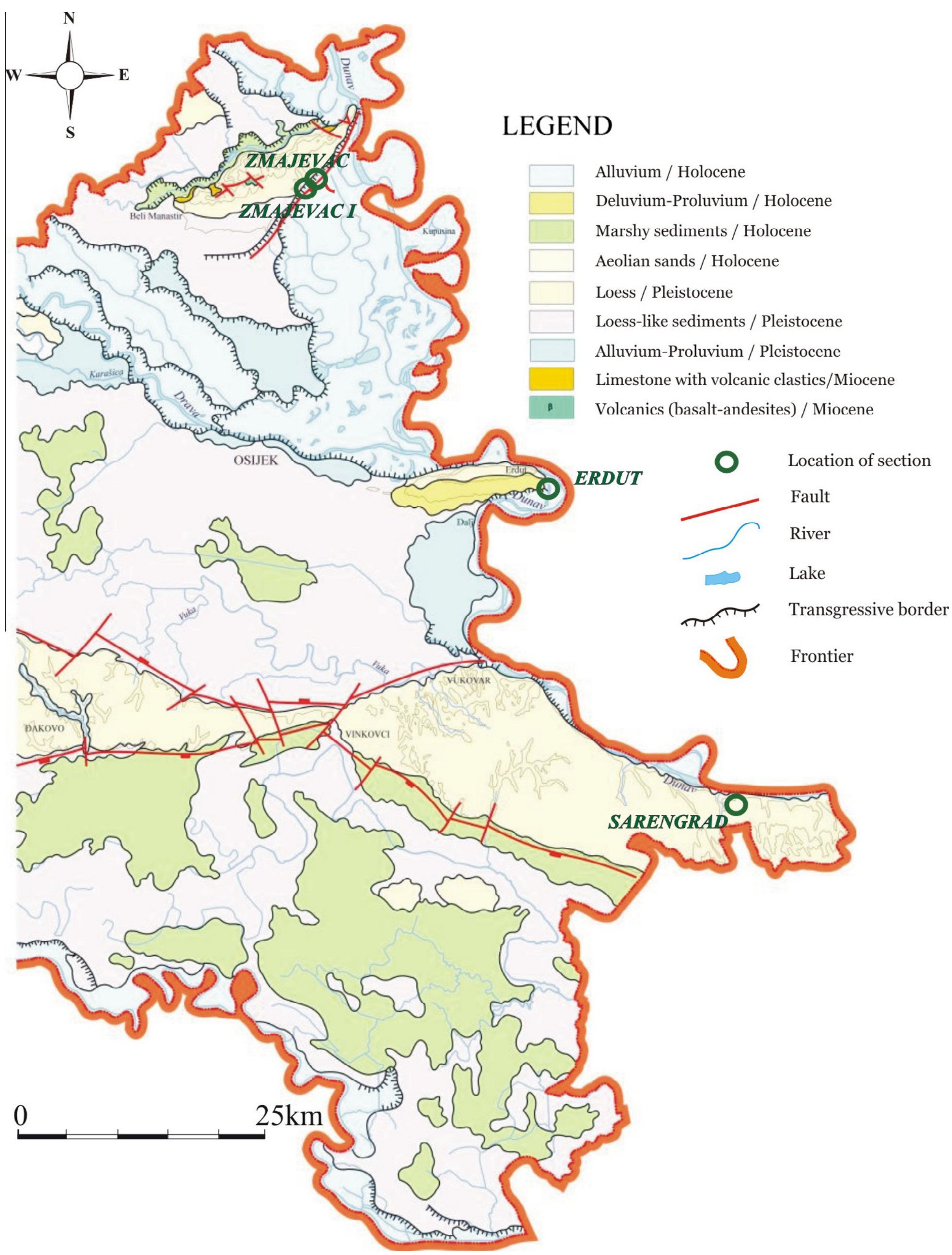

Fig. 2. Geological map of the Eastern Croatia (CGS-Department for Geology, 2009) showing the position of the sections.

2.1.1. Zmajevac I section

The Zmajevac I section (45°48′37″ N., 18°49′02″ E) is about one kilometer to the NE from the center of Zmajevac (Fig. 1) at the elevation of about 95 m asl. The total thickness of the sediment succession is between 6 and 8 m but only 5.5 m of the bottom part was available to study.

Loess is deposited at the bottom of the investigated profile. The oldest exposed paleosol is reddish-brown well-developed hydromorphic soil, covered by laminated alluvial sediments composed of eroded well-developed paleosol and loess. The upper erosional boundary is overlain by accumulation of carbonate concretions, crushed carbonate coatings and fossil remains of bones and gastropod shells. The second paleosol is a brown soil while the uppermost paleosol is only weakly developed and superimposed by the recent soil. For a detailed lithostratigraphical subdivision of the profile see Galović (2014).

2.1.2. Zmajevac section

The investigated section is situated 45°48′49″ N and 18°49′33″ E, at an elevation of 90 m asl., about 2 km to the NE of the village of Zmajevac and about 1 km away from the Zmajevac I section (Fig. 1). The sediment succession has a thickness of 28.5 m (Fig. 3).

On top of the loess sediment is a layer of carbonate concretions up to 50 cm in diameter, followed by loess and a layer of platy carbonate concretions. The upper Ck-horizon is covered by loess that yielded IRSL age estimate of 217 ± 22 ka (OIS 8). The upper boundary is covered by accumulations of the gastropod detritus and carbonate-rich material in the form of the lens-like structures. This horizon is overlain by the brown pedocomplex followed by loess, with IRSL age estimate of 121 ± 12 ka (OIS 6) and another pedocomplex (double soil) intercalated by laminated sediment. The whole succession is overlain by another loess horizon. Two samples taken from loess yielded IRSL age estimates of 101 ± 10 and 68.6 ± 6.9 ka. A well-developed brown paleosol (OIS 5) is exposed above the loess qnd followed by a weakly developed paleosol (OIS 3) about 205 cm thick. This paleosol is covered by loess and overlain by a modern rendzina soil at the top of the section. The stratigraphically youngest loess gave IRSL age estimates ranging from 16.7 ± 1.8 to 20.2 ± 2.1 ka (OIS 3). For a detailed lithostratigraphical subdivision of the profile see Galović (2014).

2.2. Erdut section

The Erdut section (45°30′49″ N, 19°04′57″ E) is located in front of the bridge crossing the Danube River near the village of Erdut (Fig. 1), at an elevation of about 100 m asl. The sediment succession has a thickness of about 22 m (Fig. 3).

At the bottom of the investigated profile loess is covered by large carbonate concretions beneath the well-developed, brown to strong brown, pedocomplex. This strongly developed pedocomplex is covered by soil with weak humification. The overlaying loess layer gave IRSL age estimate of 61.5 ± 6.2 ka. The upper part of the loess horizon is truncated and covered by laminated alluvial sediments. The upper boundary is covered by a horizon of broken gastropod shells and secondary carbonate concretions in the form of small lenses.

Loess covering the alluvial sediments yielded IRSL age estimate of 53.8 ± 5.4 ka. Weakly developed paleosol is covered by porous loess (IRSL age estimates of 46.5 ± 4.7 ka and of 46.9 ± 4.8 ka). The carbonate-free loess is superimposed by a dark yellowish brown paleosol. IRSL age estimate of 19.8 ± 2.1 ka was determined for the stratigraphically youngest loess layer. For a detailed lithostratigraphical subdivision of the profile see Galović (2014).

2.3. Šarengrad

The Šarengrad section (45°13′21″ N, 19°17′50″ E) is situated in a road cut, about one kilometer east of the center of Šarengrad (Fig. 1). The elevation is about 110 m asl. (Fig. 3). The 16 m thick loess–paleosol sequence has been described in detail by Galović et al. (2011).

The oldest hydromorphic paleosol contains Fe/Mn-precipitates. The lowermost loess horizon has a thickness of 140 cm and gave an IRSL age estimate of 86.6 ± 8.6 ka. This layer is truncated and covered by laminated sediment with wave-ripple marks in the lower part. The well-developed argillic dark brown paleosol is characterised by rubification and illuviation processes. The loess on top of the paleosol is covered by another brown paleosol. The up permost paleosol is weakly developed and covered by loess, which is influenced by recent pedogenesis. IRSL age of 55.3 ± 5.5 ka estimated for the uppermost loess can be correlated to the OIS 3–4.

3. Sampling and methods

After removing a half of meter of outcrop in order to reduce influence of weathering and vegetation, based on field observations (color, grain size, structure, texture, bioturbations, presence and form of carbonates ...) 110 horizons were defined. The total of 110 samples was described (Galović et al., 2009; Galović, 2014) and collected from the loess, paleosols and alluvial sediments at the four different sections to determine their mineralogical composition (Table 1).

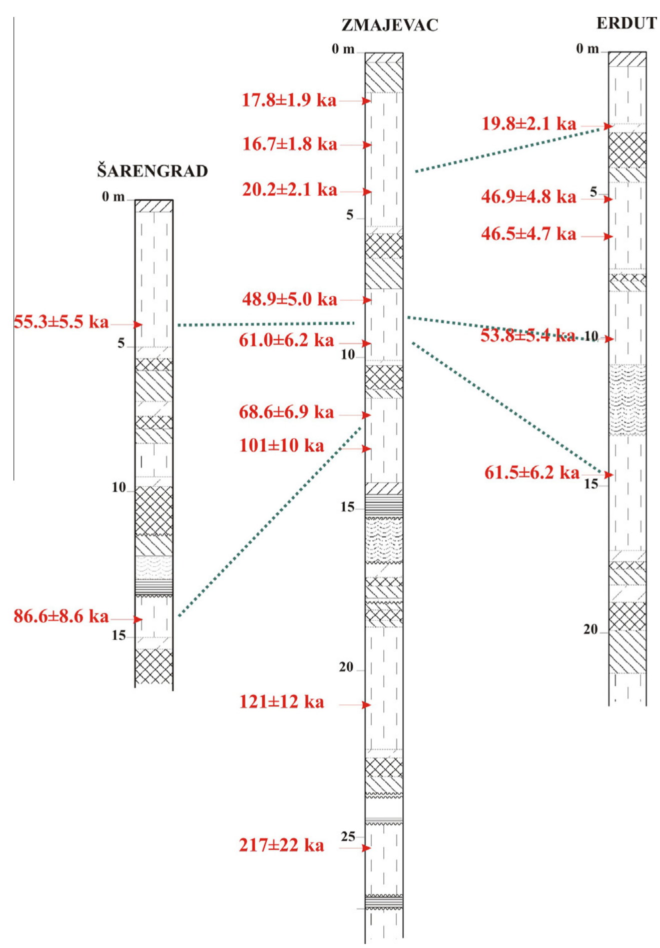

Fig. 3. Luminescence dating results of the Šarengrad, Zmajevac and Erdut sections (retrieved from Galović et al. (2009)).

Table 1
List of samples, depths of sampling and colors of horizons (Munsell Soil Color Charts, 2000).

Sample	Depth (cm)	Color
Zmajevac		
Z-1	130–330	2.5Y6/4
Z-2	400–520	2.5Y6/4
Z-3	520–570	2.5Y6/4
Z-4	570–595	2.5Y6/4
Z-5	595–655	10YR5/4
Z-6	655–675	10YR5/4
Z-7	675–775	2.5Y5/4
Z-8	775–990	2.5Y7/2
Z-9	990–1010	2.5Y6/4
Z-10	1010–1027	2.5Y6/4
Z-11	1027–1035	10YR5/4
Z-12	1035–1055	10YR4/4
Z-13	1055–1067	10YR4/3
Z-14	1067–1090	10YR4/3
Z-15	1090–1105	10YR4/4; 10YR6/4
Z-16	1105–1135	10YR6/4
Z-17	1135–1200	2.5Y6/4
Z-18	1200–1225	2.5Y6/4
Z-19	1225–1300	2.5Y6/4
Z-20	1450–1500	2.5Y6/4
Z-21	1500–1680	2.5Y6/4
Z-22	1680–1730	2.5Y6/4
Z-23	1730–1760	10YR4/4
Z-24	1760–1800	10YR6/6
Z-25	1800–1815	7.5YR5/4
Z-26	1815–1840	10YR5/4
Z-27	1840–1875	10YR4/4
Z-28	1875–1897	10YR6/4
Z-29A	1897–1957	2.5Y6/4
Z-29B	2047–2262	2.5Y6/4
Z-30	2262–2287	2.5Y7/2
Z-31	2287–2311	2.5Y6/4
Z-32	2311–2326	10YR5/4
Z-33	2326–2373	10YR5/4
Z-34	2373–2403	7.5YR4/5
Z-35	2403–2461	7.5YR4/6
Z-36	2461–2472	10YR5/4
Z-37	2472–2503	10YR5/6
Z-38	2503–2543	5Y7/4
Z-39	2543–2556	5Y7/4
Z-40	2556–2564	7.5YR4/4
Z-41A	2564–2664	2.5Y6/4
Z-41B	2664–2804	2.5Y6/4
Z-42	2804–2850	2.5Y6/4
Erdut		
E-1	200–247	2.5Y7/2
E-2	247–278	2.5Y7/3
E-3	278–307	2.5Y5/4
E-4A	307–350	10YR4/4
E-4B	350–400	10YR4/4
E-5	400–450	2.5Y5/4
E-6	450–530	2.5Y5/4
E-7	700–750	2.5Y6/4
E-8	750–767	10YR5/4
E-9	767–790	10YR5/4
E-10	790–826	10YR6/4; 2.5Y7/3
E-11	826–856	2.5Y7/3
E-12A	856–906	2.5Y7/3
E-12B	986–1076	2.5Y7/3
E-13A	1080–1120	2.5Y7/3
E-13B	1120–1320	2.5Y6/4; 2.5Y7/2
E-14A	1320–1370	2.5Y7/3
E-14B	1690–1720	2.5Y7/3
E-15	1720–1760	2.5Y6/4
E-16	1760–1785	2.5Y6/4
E-17	1785–1840	2.5Y6/4
E-18	1840–1900	2.5Y7/3
E-19	1900–1945	10YR4/4; 7.5YR4/4
E-20	1945–1997	7.5YR4/6
E-21A	1997–2009	7.5YR4/6
E-21B	2009–2057	7.5YR4/6
E-22	2057–2085	7.5YR4/4
E-23	2085–2145	2.5Y7/3
E-24	2145–2200	2.5Y7/3
Šarengrad		
Š-1	400–500	2.5Y7/3
Š-2	500–526	10YR6/4
Š-3	526–543	10YR6/4
Š-4	543–581	10YR6/4
Š-5	581–607	10YR5/4
Š-6	607–687	10YR5/4
Š-7	687–702	10YR6/4
Š-8	702–737	7.5YR5/3
Š-9	737–780	10YR5/4
Š-10	780–830	2.5Y5/4
Š-11	830–944	2.5Y7/3
Š-12	944–959	10YR6/4
Š-13	959–977	10YR5/4
Š-14	977–995	7.5YR5/4
Š-15	995–1018	7.5YR4/4
Š-16	1018–1057	7.5YR4/3
Š-17A	1057–1082	7.5YR4/4
Š-17B	1082–1142	7.5YR4/4
Š-18	1142–1214	2.5Y7/3
Š-19	1214–1294	2.5Y6/6; 2.5Y4/4
Š-20	1294–1352	2.5Y6/6; 2.5Y4/4
Š-21	1352–1361	2.5Y6/3
Š-22	1361–1492	2.5Y6/4
Š-23	1492–1512	10YR5/4
Š-24	1512–1532	10YR5/4
Š-25	1532–1550	10YR5/6
Š-26	1550–1620	10YR4/6

Samples were air-dried for approximately one month period. After drying, the samples were sieved to the <2 mm fraction to separate the sediment from larger carbonate concretions, while smaller, if present, remained in the samples (Galovic et al., 2011).

3.1. Modal analyses

To determine the qualitative and semi-quantitative mineral composition of heavy and light mineral associations, 110 samples were extracted after disaggregation in the ultrasonic bath and sieved to the 0.09–0.16 mm size fraction, followed by the subsequent dissolution of calcite. This fraction was selected for the analysis because it includes all virtual mineral species in proportions representative for the bulk sample. The heavy mineral fraction (HMF) was separated using bromoform ($CHBr_3$) at a density of 2.85–2.88 gcm^{-3}. Slides of heavy and light mineral fraction (LMF) were examined in the polarized light. Qualitative and semi-quantitative composition of a sample was established after the determination of 300–400 grains and the percentage of each mineral was calculated. Canada balsam was used as the mounting medium.

3.2. Morphologic observations

Specific shapes of mineral grains were visible on grain surfaces under magnification 200× using polarization microscope. Aeolian transport is characterized by mutual punching of grains in the air, causing much abraded rounded grains with punctuated surfaces. Alluvially transported grains have sharp edges caused by breakage during crashing in dense media (water).

Up to now, most of morphologic compartions on shape, habitus and abrasion marks of grains transported by wind and/or water were accomplished by analyzing quartz grains because they are generally the most frequent minerals in loess and chemically resistant. Since muscovite is a frequent mineral in analyzed samples

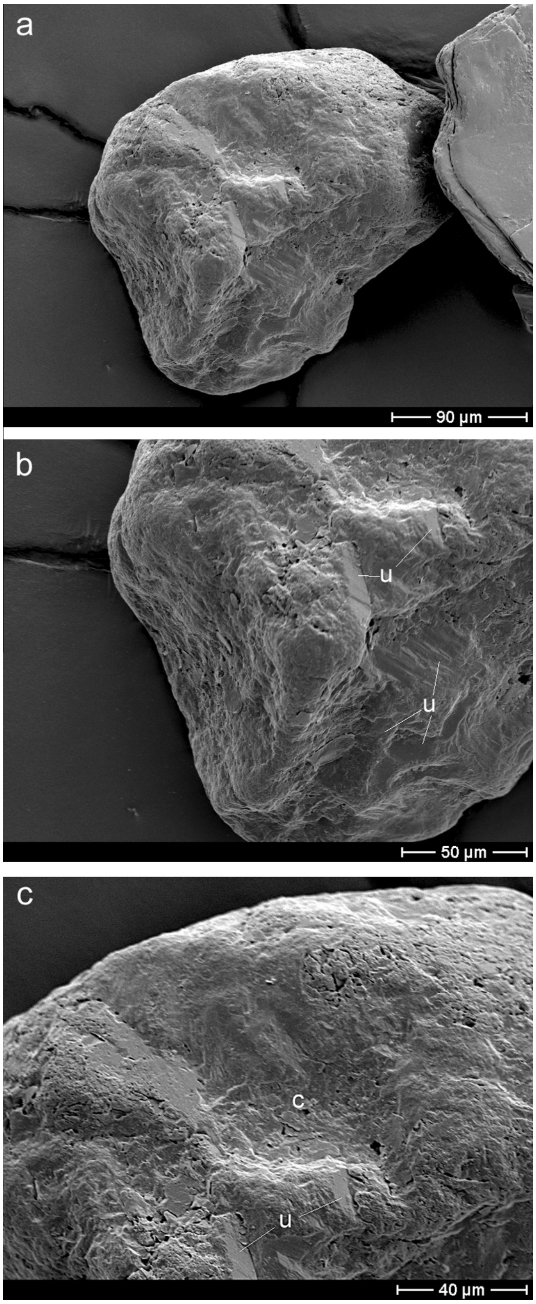

Fig. 4. Typical aeolian micro textures are visible: c-concave depressions, u-upturned plates and rounded edges. Sample Š-11.

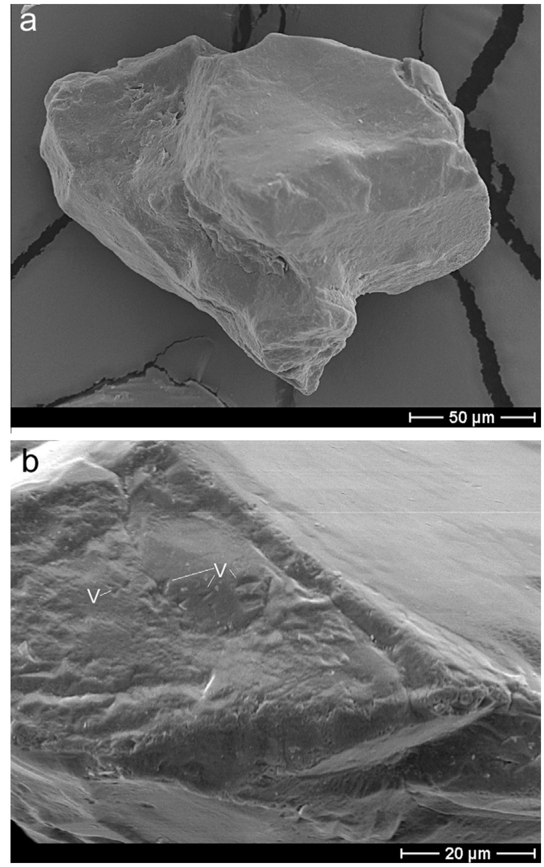

Fig. 5. Aeolian transported quartz grains, reworked by fluvial transport indicated with: (a) Concave depressions and rounded edges indicating aeolian transport; (b) V-shaped patterns indicating fluvial rework. Sample Z-20.

and resistant to chemical weathering as well, muscovite plates were analyzed simultaneously.

Morphologic observations of samples were carried out with the JEOL JSM-35F scanning electron microscope (SEM), operating in secondary electron (SE) mode at an accelerating voltage of 10 kV. The grains were mounted on the SEM stubs and sputtered with gold.

4. Results and discussion

4.1. Morphological characteristic of analyzed grains

The basic morphological characteristic of analyzed grains is high spherical rounded hypidiomorphic to allotriomorphic grains. This is the most noticeable in rounded habitus of typical (hyp)idiomorphic crystals like tourmaline and zircon. Sphericity and roundness of grains indicate the type of abrasion. Namely, alluvially transported grains have some sharp edges caused by breakage during crashing in dense media (water). They are characterized by parallel striations, whilst aeolian transport is characterized by mutual punching of grains in the air, causing very abraded rounded grains with punctuated surfaces (Ujházy et al., 2003).

Based on roundness of kyanite, it can be concluded that mechanical abrasion was strong enough for rounding the kyanite grains, but not too strong to crush them, or break them along their cleavage planes. Well rounded mica and chlorite leaflets indicate slow wind (Mutić, 1990). Abrasion has been dominating over chemical weathering, because minerals less resistant to weathering (for example amphibole) are present in all analyzed horizons. Apart from the detrital grains, idiomorphic crystals of volcanogenetic minerals with preserved crystallographic forms can be occasionally found (zircon, rutile, and biotite).

Aeolian deposited sections contain well rounded quartz grains with micro textures indicating material transport by wind. Numerous concave, elongated or equidimensional depressions can be found on the grains surface. Grain edges are well rounded and so called upturned plates textures are common (Fig. 4).

On the loess grains from the laminated sections; finally transported in aquatic system numerous aeolian micro textures still can be found. This can be explained with relatively short aquatic transport or with low water energy conditions. In the fluvial redeposited quartz grains original aeolian marks are often excellently preserved due to quartz mechanical and chemical resistivity.

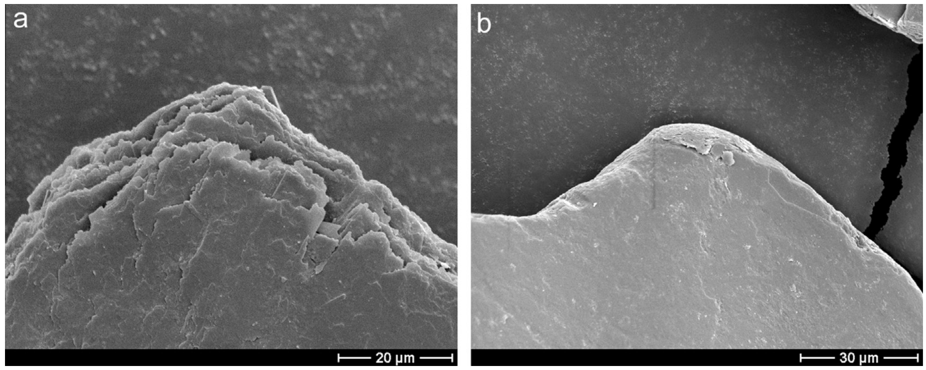

Fig. 6. (a) The fluvial muscovite grain with micro fractured edge and rough blocky surface. (b) The aeolian muscovite grain with rounded edge and smoothed surface.

Table 2
Modal compositions of the heavy and light mineral fractions.

Sample	Comp. of LMF 100%				% of HMF	Comp. of HMF 100%				Comp. of THM 100%											
	q	f	m	l		op	co	b	THM	ep–zt	am	py	g	cy	st	tu	zr	ru	ti	ap	cr
Zmajevac																					
Z-1	73	10	10	6	3.74	24	6	2	68	13	17	3	46	2	3	5	4	2	4	1	2
Z-2	60	13	13	14	4.09	8	15	3	73	20	29	5	25	2	6	5	1	+	2	3	+
Z-3	47	11	36	6	4.5	7	36	25	33	13	36	4	33	3	3	4	0	1	2	1	0
Z-4	42	10	35	13	4.9	4	43	20	33	16	30	5	26	5	7	6	1	1	3	0	2
Z-5	60	14	18	8	5.1	7	27	13	53	19	33	2	25	5	5	6	2	1	1	2	0
Z-6	57	19	13	12	5.48	4	25	4	68	22	36	6	22	2	6	2	1	+	+	0	2
Z-7	55	16	20	9	3.8	16	30	5	49	14	37	2	24	2	5	4	4	1	3	4	0
Z-8	7	3	87	3	3.0	6	36	27	30	14	39	3	17	4	11	2	2	2	5	1	0
Z-9	27	6	59	9	3.5	8	35	19	38	20	32	3	23	3	10	5	0	1	3	1	0
Z-10	24	8	61	7	3.7	10	36	21	33	20	36	5	20	2	9	6	1	0	1	0	1
Z-11	63	19	13	5	5.61	8	16	3	73	28	37	8	19	2	2	0	3	2	0	0	0
Z-12	44	10	39	7	4.1	8	24	16	52	30	24	3	24	5	3	3	1	1	3	3	0
Z-13	67	12	12	9	7.37	13	12	1	74	29	26	4	27	3	4	1	2	2	1	0	0
Z-14	70	12	4	14	2.3	9	22	1	67	23	22	4	29	4	5	7	1	1	3	2	0
Z-15	66	20	6	8	6.39	11	6	1	83	32	23	6	28	1	4	2	2	2	1	0	0
Z-16	71	17	6	6	1.0	7	29	4	61	18	37	1	29	1	4	3	2	1	4	0	0
Z-17	59	12	20	9	<0.1	9	30	5	56	15	15	1	36	2	4	4	6	7	4	6	1
Z-18	58	11	16	15	2.71	9	22	3	66	27	20	7	32	1	1	3	3	2	2	+	+
Z-19	59	17	14	11	3.82	7	23	2	68	30	18	7	32	3	6	2	2	2	+	0	0
Z-20	34	7	54	5	2.0	2	41	21	36	16	22	10	27	2	5	8	5	0	3	3	1
Z-21	28	5	66	2	<0.1	1	52	17	30	37	17	6	14	6	6	2	1	1	3	5	3
Z-22	26	4	68	2	6.2	1	57	19	24	17	34	7	14	5	4	4	3	0	7	3	1
Z-23	83	7	5	4	3.5	18	3	1	78	27	24	4	27	2	6	3	1	2	2	2	0
Z-24	64	12	19	5	3.6	4	16	3	77	24	31	2	26	4	6	2	0	1	3	0	1
Z-25	76	11	8	6	3.6	16	5	3	77	22	18	7	34	4	4	5	2	+	3	1	+
Z-26	76	10	8	6	3.3	7	5	2	86	25	13	3	33	8	7	3	2	1	2	3	1
Z-27	75	13	5	7	5.0	5	10	4	81	20	18	4	37	3	6	5	+	1	4	1	1
Z-28	73	9	8	10	4.3	+	5	4	91	22	19	2	39	3	5	3	2	1	3	1	0
Z-29A	68	12	15	5	4.4	5	17	3	75	18	22	4	36	3	6	3	1	1	2	1	2
Z-29B	54	8	28	10	1.5	12	29	12	47	14	18	0	30	15	9	3	2	4	3	2	1
Z-30	34	5	55	5	9.2	6	35	4	55	16	40	2	26	2	1	1	2	1	2	3	3
Z-31	58	6	29	7	8.9	4	24	3	68	15	27	1	36	5	3	2	2	3	1	2	2
Z-32	53	7	35	5	4.3	3	36	2	59	15	24	2	39	1	3	5	1	+	4	2	3
Z-33	81	10	3	7	3.2	9	4	4	83	9	7	1	62	2	5	5	1	3	4	1	+
Z-34	82	9	5	4	3.9	18	4	1	78	14	12	0	53	6	3	3	1	2	2	3	+
Z-35	79	7	10	4	3.3	16	5	2	77	17	15	1	54	3	4	3	0	2	1	+	+
Z-36	76	10	7	7	6.5	6	13	4	77	10	23	1	51	2	2	3	1	2	1	1	1
Z-37	74	10	7	9	9.3	6	8	4	82	13	19	1	50	2	4	4	+	1	2	3	+
Z-38	70	6	13	11	4.8	6	37	14	43	17	28	1	34	6	3	3	1	3	1	2	0
Z-39	19	3	75	3	5.7	2	56	17	25	24	24	1	27	4	3	4	4	2	0	5	1
Z-40	16	1	82	1	3.2	4	35	13	48	18	29	1	35	2	3	6	1	3	1	1	0
Z-41A	16	2	80	2	2.5	5	46	33	17	26	8	3	31	3	3	3	3	3	13	2	2
Z-41B	10	2	86	2	4.0	1	43	48	7	43	13	0	22	4	4	0	0	9	4	0	0
Z-42	16	3	75	6	5.0	5	43	33	19	15	33	0	26	5	5	5	0	2	5	2	3
Zmajevac I																					
ZI-1	78	9	7	6	4.3	11	12	2	75	11	36	4	20	9	10	3	3	1	2	0	0
ZI-2	76	14	5	6	3.6	6	9	1	85	17	26	2	34	5	8	3	2	2	1	2	0
ZI-3	71	11	12	6	7.5	11	2	3	85	11	36	1	30	4	5	1	5	2	3	2	0
ZI-4	78	14	3	5	5.6	19	2	2	78	8	24	2	46	5	7	1	2	3	+	+	1
ZI-5	77	8	11	4	4.0	17	7	4	72	18	18	1	30	5	9	3	6	4	2	+	4

(continued on next page)

Table 2 (*continued*)

Sample	Comp. of LMF 100%				% of HMF	Comp. of HMF 100%				Comp. of THM 100%											
	q	f	m	l		op	co	b	THM	ep–zt	am	py	g	cy	st	tu	zr	ru	ti	ap	cr
ZI-6	69	13	6	12	10.0	14	7	3	77	15	20	1	42	6	5	2	5	2	2	1	1
ZI-7	68	11	9	12	7.5	7	4	2	87	11	21	3	45	5	4	4	2	2	2	1	+
ZI-9	80	10	2	8	8.2	15	+	1	84	7	8	3	65	3	2	6	2	3	1	0	0
ZI-10	77	10	6	7	<0.1	29	8	12	51	19	5	4	38	5	5	5	7	3	4	4	1
ZI-11	64	10	21	5	<0.1	+	24	68	7	4	20	4	28	8	4	12	8	4	4	4	0
Erdut																					
E-1	44	3	51	2	3.2	10	35	8	47	18	25	2	25	1	9	8	1	3	3	2	2
E-2	67	5	23	5	3.8	10	20	7	63	19	22	4	29	2	5	5	3	2	3	2	3
E-3	63	12	17	8	4.2	12	18	4	67	21	30	1	26	2	3	4	+	3	4	4	1
E-4A	59	21	8	12	14.78	13	5	1	81	28	26	2	29	1	3	1	2	6	1	0	0
E-4B	69	8	17	6	3.2	8	16	3	73	19	24	2	30	3	3	7	4	2	3	1	+
E-5	46	4	43	8	3.1	7	20	4	70	14	35	+	33	1	6	3	1	2	1	1	0
E-6	27	3	67	3	3.5	8	31	8	54	19	34	2	34	2	2	1	0	1	3	1	1
E-7	33	4	62	2	4.8	2	26	18	54	23	36	2	26	7	1	1	2	1	2	0	0
E-8	46	7	41	5	6.2	2	27	18	52	17	26	1	35	5	5	4	3	1	3	1	0
E-9	46	6	45	3	4.5	8	16	3	73	19	24	2	30	3	3	7	4	2	3	1	+
E-10	74	14	4	7	3.3	12	23	8	57	14	23	3	44	3	4	3	1	2	3	0	0
E-11	54	5	35	6	3.9	21	18	17	43	18	15	2	44	2	4	3	3	3	1	4	1
E-12A	67	16	6	11	11.58	26	3	1	70	17	12	5	44	1	7	2	5	5	1	0	1
E-12B	42	15	20	23	14.67	5	11	7	78	20	31	5	33	+	4	+	1	4	2	0	0
E-13A	57	11	10	22	17.49	7	12	1	80	17	27	10	34	0	3	2	4	2	1	0	1
E-13B	53	23	9	15	15.89	6	3	0	91	23	19	9	41	0	2	0	1	2	2	0	0
E-14A	63	15	2	20	5.82	10	10	1	79	26	29	6	31	1	4	2	1	1	0	0	0
E-14B	60	10	26	4	3.8	3	20	6	71	22	35	4	20	3	4	3	2	0	3	2	2
E-15	58	8	27	6	4.0	17	14	7	62	20	34	3	27	3	5	2	1	+	1	1	1
E-16	54	8	32	6	3.9	10	26	10	53	25	35	1	19	2	7	4	0	1	2	4	1
E-17	59	8	26	7	4.0	18	13	5	64	26	17	2	36	4	7	4	2	+	2	0	0
E-18	61	10	24	5	4.6	9	9	4	79	19	24	3	30	5	4	5	+	3	5	2	1
E-19	69	18	4	9	13.69	6	1	+	93	38	13	6	34	1	5	2	1	1	1	0	0
E-20	72	14	9	5	4.3	8	5	2	85	17	19	3	44	2	5	2	3	2	2	+	1
E-21A	69	15	1	15	4.8	16	8	2	75	17	25	2	40	2	5	3	1	2	2	+	0
E-21B	72	15	5	8	13.87	8	4	0	88	31	13	5	33	1	7	2	2	5	+	0	0
E-22	68	7	19	6	3.7	22	15	2	61	17	24	2	40	1	4	1	3	1	3	2	1
E-23	55	13	20	12	4.15	11	21	+	68	33	17	5	33	1	6	1	2	2	+	0	0
E-24	42	4	51	4	11.2	9	49	13	29	19	35	1	33	2	1	5	1	2	0	0	0
Šarengrad																					
Š-1	21	2	72	4	4.8	13	43	16	28	26	16	5	33	1	2	2	3	3	5	1	1
Š-2	53	12	26	9	4.04	7	22	2	68	27	31	11	22	0	3	1	1	2	1	0	0
Š-3	74	8	15	3	4.5	20	14	6	60	23	22	2	34	2	3	5	2	3	2	1	+
Š-4	60	8	26	7	4.8	10	20	5	64	22	23	2	32	2	3	8	3	2	+	1	+
Š-5	56	32	8	4	4.8	16	17	6	61	25	24	3	28	7	3	2	1	4	3	1	2
Š-6	56	11	30	4	3.76	11	13	3	73	36	25	7	22	1	4	1	1	3	+	0	0
Š-7	64	20	7	9	10.79	10	8	1	82	31	28	5	23	1	5	+	1	3	3	0	0
Š-8	68	8	19	4	4.2	19	23	11	46	24	23	5	35	1	6	1	1	2	1	1	1
Š-9	63	9	21	7	3.0	14	29	6	51	26	9	4	34	4	5	3	3	5	3	0	3
Š-10	33	4	59	3	3.5	9	37	14	40	19	16	3	39	4	4	5	2	2	6	1	0
Š-11	20	6	71	3	4.59	9	37	14	40	31	20	6	33	0	3	1	1	1	3	0	0
Š-12	35	2	61	1	3.0	15	35	15	35	25	9	2	33	5	4	2	3	6	5	0	6
Š-13	61	13	11	15	6.74	21	6	1	73	17	8	20	40	1	4	1	5	5	1	0	0
Š-14	72	15	11	2	4.0	48	6	2	44	21	10	3	37	3	4	6	2	4	5	0	5
Š-15	72	13	7	7	3.33	30	4	1	66	25	18	11	31	5	3	1	3	2	0	1	0
Š-16	77	17	4	2	5.0	61	10	1	28	16	16	7	33	4	5	3	6	5	4	0	0
Š-17A	73	12	10	5	2.5	58	7	4	32	18	10	4	38	8	8	4	1	4	1	3	1
Š-17B	76	12	4	9	2.53	25	3	+	72	38	4	4	36	0	5	3	+	4	2	2	1
Š-18	46	11	42	2	5.13	12	32	1	55	22	10	18	37	0	1	2	2	5	1	0	1
Š-19	32	8	53	7	7.38	9	44	11	36	28	23	21	16	0	5	4	1	1	0	0	0
Š-20	34	9	53	3	10.58	19	42	7	33	20	24	10	30	0	1	3	1	7	1	0	1
Š-21	35	8	49	9	5.31	8	36	4	53	20	25	8	30	4	6	2	1	1	2	0	1
Š-22	47	11	40	2	6.0	51	24	3	23	17	14	3	33	3	5	3	2	1	7	3	7
Š-23	30	9	59	3	7.73	7	57	7	29	26	6	18	32	0	6	7	3	2	0	0	1
Š-24	53	27	16	4	3.3	37	19	2	42	5	4	10	36	3	1	2	0	2	18	18	0
Š-25	35	7	54	3	4.61	16	24	2	58	35	13	18	21	0	3	1	1	1	5	4	2
Š-26	78	14	3	5	<0.1	34	4	3	59	32	5	6	14	7	2	6	5	3	14	5	2

LMF = light mineral fraction, HMF = heavy mineral fraction, THM = transparent heavy minerals, q = quartz, f = feldspar, m = muscovite, l = transparent lithic particles, op = opâque minerals, ch = chlorite, b = biotite, ep–zt = epidote–zoisite, am = amphibole, py = pyroxene, g = garnet, cy = kyanite, st = staurolite, tu = tourmaline, zr = zircon, ru = rutile, ti = titanite, ap = apatite, cr = chromite, + = minerals with occurrence <0.5%.

A typical grain from the laminated section shows micro textures characteristic for aeolian transport such as upturned plates and rounded bulbous edges. These textures are partially overprinted by fluvial abrasion. V-shaped patterns are indicating high energy grain collision (Fig. 5) usually produced due to the grain saltation during aquatic transport (Krinsley and Donahue, 1968; Mahaney et al., 2001; Mazzullo and Ritter, 1991).

To avoid this problem, much softer muscovite grains were studied. Muscovite grains, finally transported by wind can be successfully distinguished from the ones transported by aquatic media,

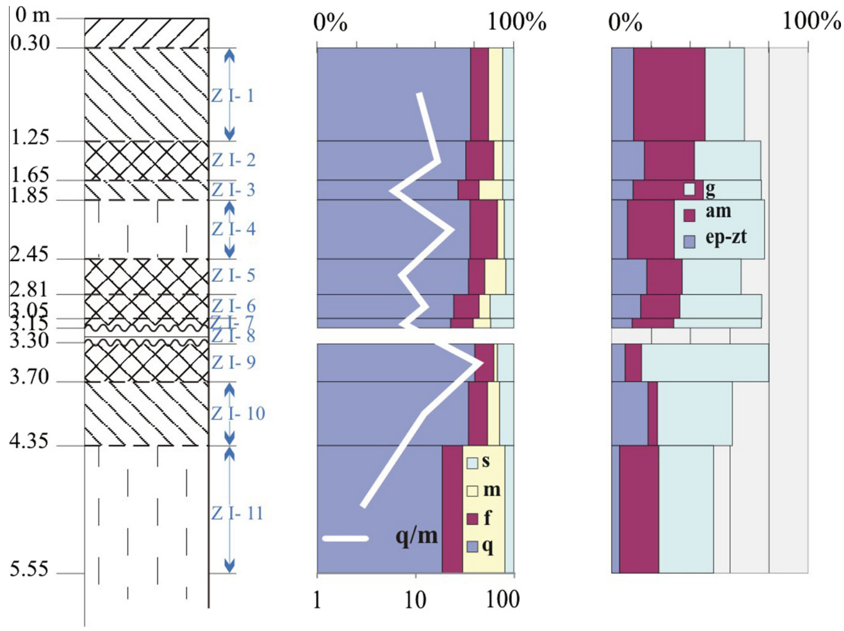

Fig. 7. Distribution of minerals of LMF and HMF along the Zmajevac I section. Legend in Table 2.

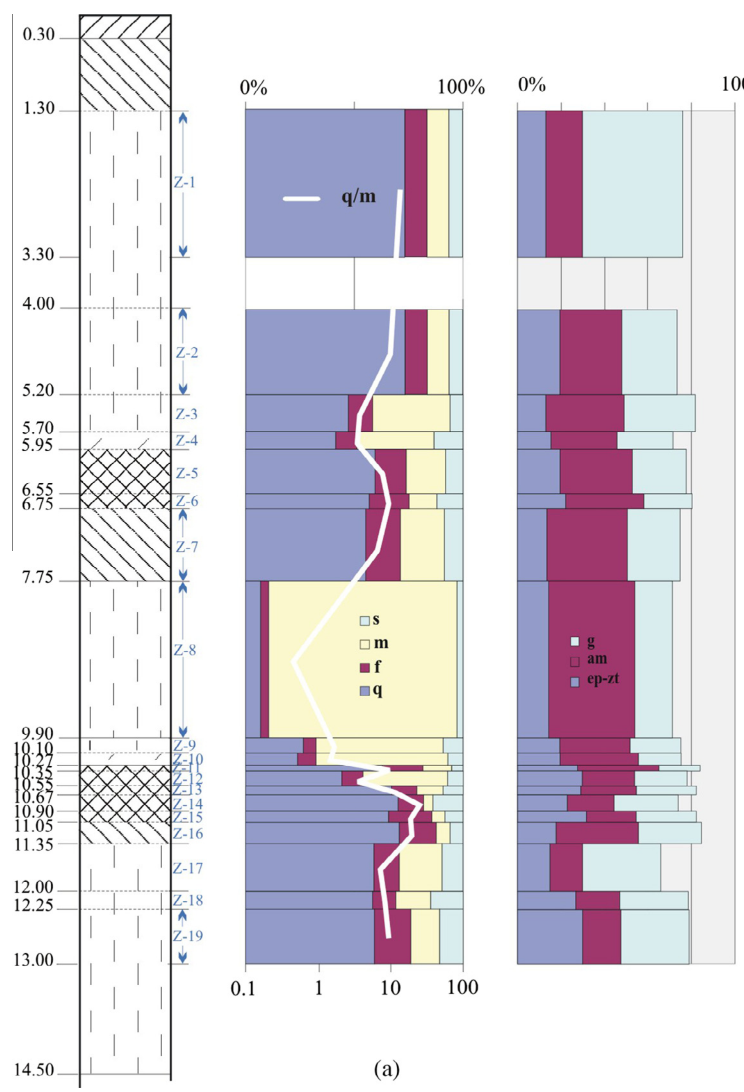

Fig. 8. Distribution of minerals of LMF and HMF along the Zmajevac section. Legend in Table 2.

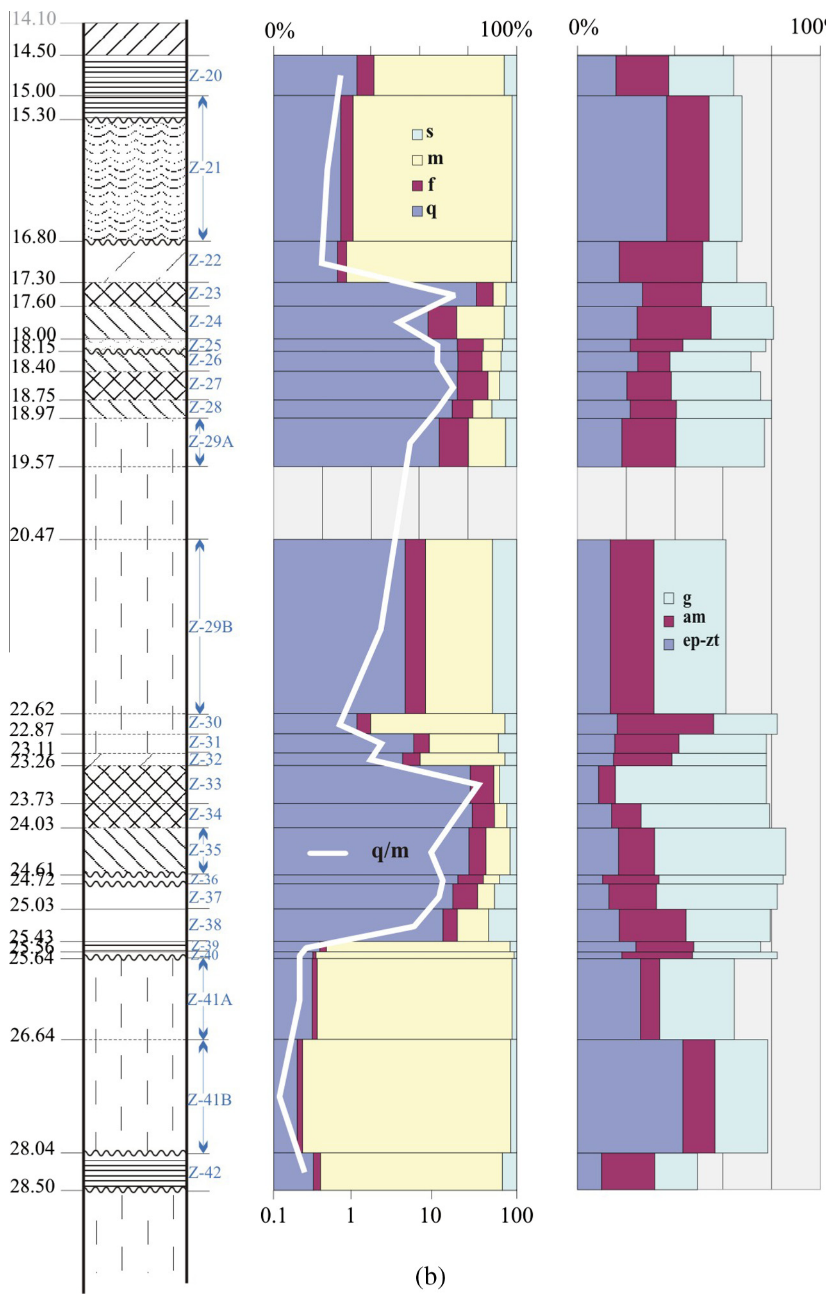

Fig. 8 (*continued*)

based on their edge and surface micro textures. The fluvial transported grains show less rounded edges with micro fractured mica plates, the surface is blocky in appearance and often covered with impact marks (Fig. 6).

The fluvial grains have nice rounded edges and smoother surface (Fig. 6). Aquatically transported grains very rarely preserve original aeolian micro textures. The usability of the muscovite grains micro textures in sediment transport interpretation is presently under experimental examination.

4.2. Composition of light mineral fraction

The results of modal analysis indicated the dominance of LMF, in comparison with heavy minerals which constitute mostly less than 10% (rarely up to 20%) of bulk mineral composition. In the Zmajevac section the rate of HMF in most horizons is <5%, whilst in the Erdut section the rate of HMF is up to 20% (Table 2). It does not depend on the impact of pedogenetic processes on investigated horizons.

The following grains were identified in the LMF of analyzed horizons: quartz, feldspar, muscovite and transparent lithic fragments (Figs. 7–10). The dominant components in the light mineral fraction are quartz (7–83%), and/or muscovite (1–87%). Their content varies significantly, since unusual enrichment of muscovite caused depletion of all other constituents of LMF. In "compositional data set" the change in content of one variable in a sample involves changes in contents of other variables of the same sample (Aitchison, 1986, 1997). Generally, quartz grains dominate in paleosol horizons, whilst muscovite dominates in loess and laminated horizons, as presented by plot quartz vs. muscovite (Figs. 7–10). Exception is the Zmajevac I section, where quartz dominates in all horizons.

Quartz and muscovite are followed by feldspars (mostly 6–12%, generally 1–32%) and lithic fragments (mostly 3–8%, generally 1–23%) (Table 2, Figs. 7–10). Feldspars are almost exclusively

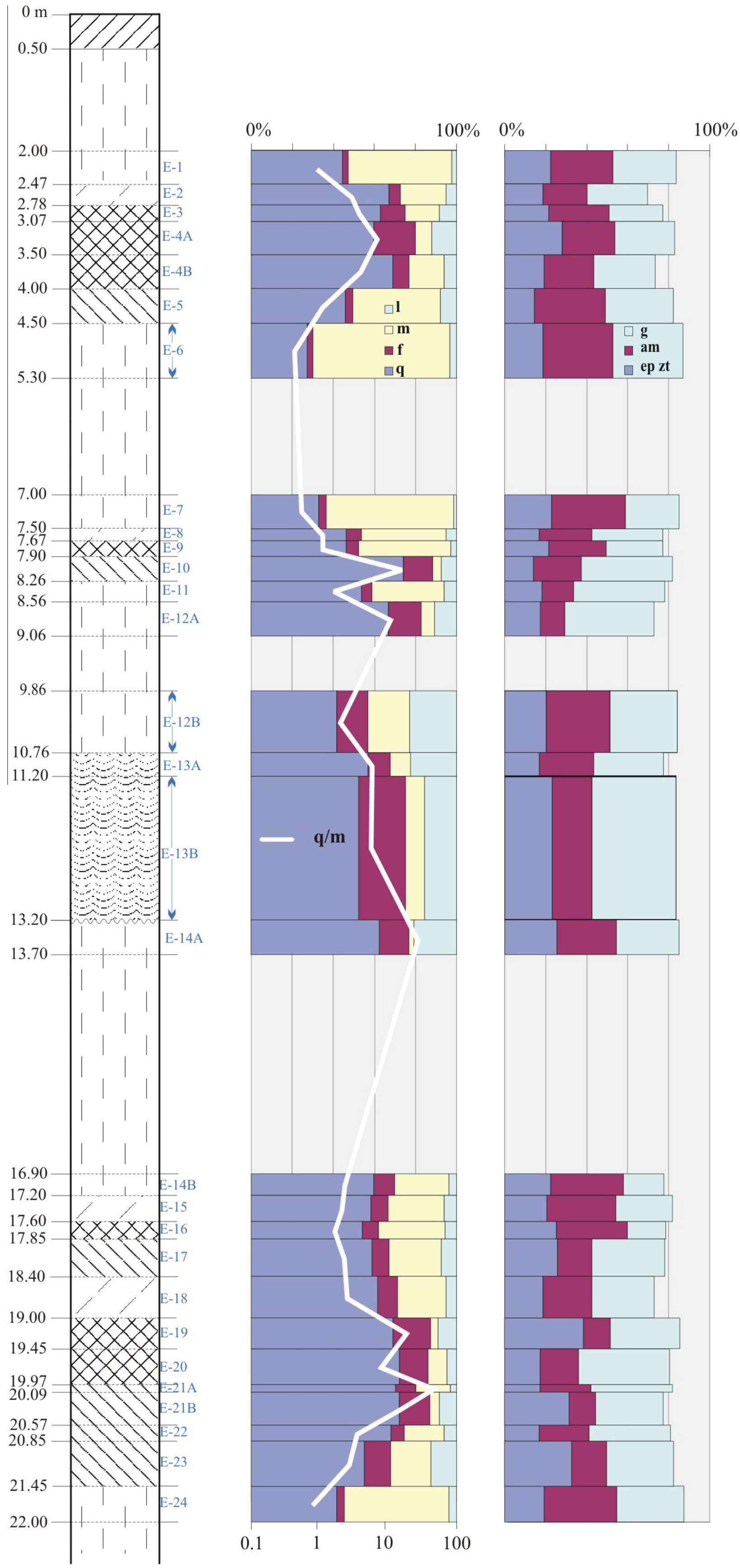

Fig. 9. Distribution of minerals of LMF and HMF along the Erdut section. Legend in Table 2.

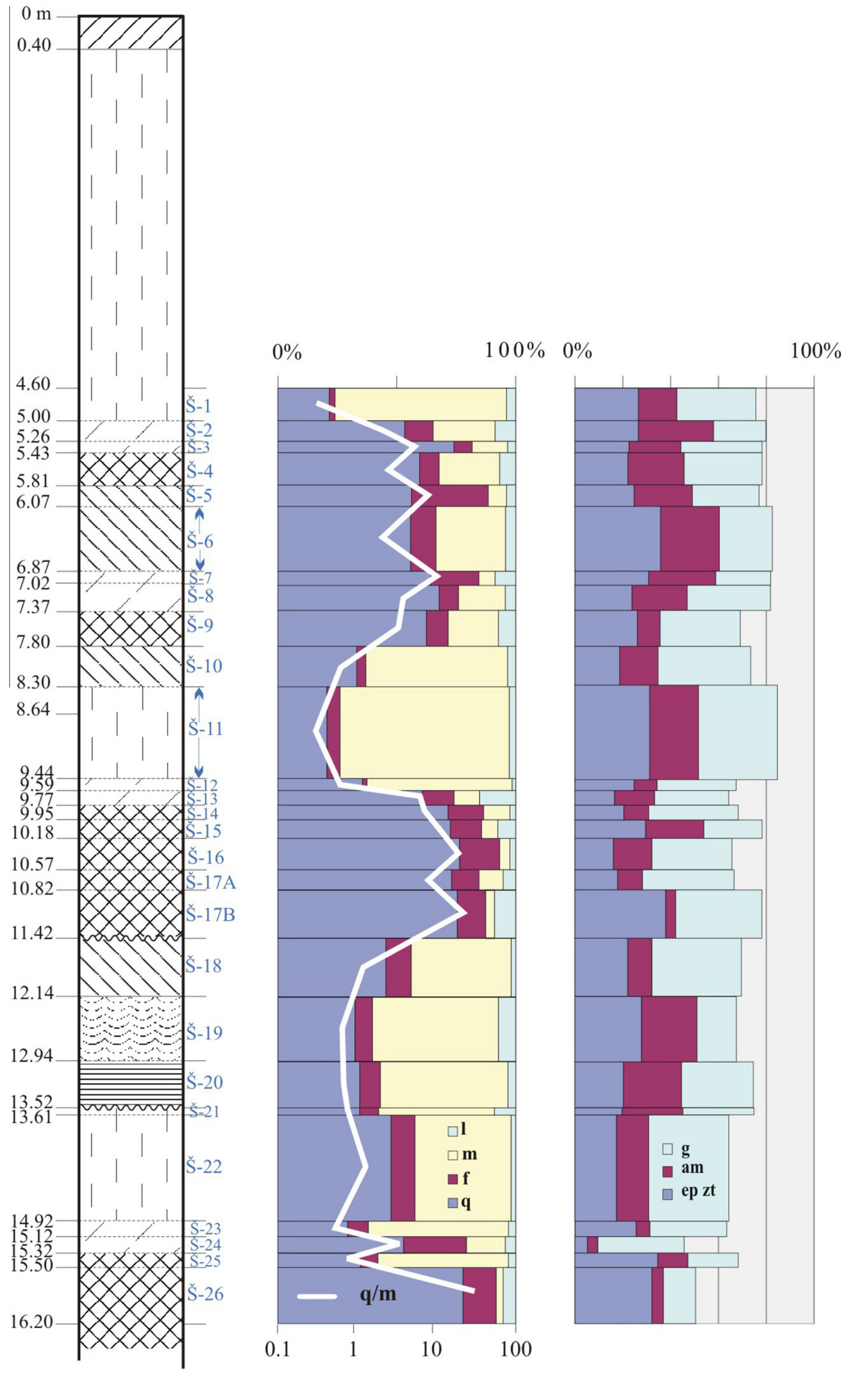

Fig. 10. Distribution of minerals of LMF and HMF along the Šarengrad section. Legend in Table 2.

presented by K-feldspars (orthoclase, rarely microcline) that are enriched in paleosols. In the Erdut and the Šarengrad sections fresh feldspar grains dominate, whilst in the Zmajevac and the Zmajevac I sections there is a similar rate of fresh and weathered grains. Lithic fragments are most often presented by quartzite, sometimes covered by sericite or limonitic coating. Other types of lithic fragments are accessory.

4.3. Composition of heavy mineral fraction

Among HMF, the transparent mineral fraction (TMF) predominates over opaque minerals in most horizons (Table 2). Exceptions are horizons of two the oldest (and pedogenetically the best developed) paleosols in the Šaregrad section, enriched in Fe-minerals (magnetite and haematite in the upper paleosol, or Fe/Mn-oxide/hydroxide concretions up to 5 mm in diameter in the oldest paleosol).

Biotite and chlorite are present in all samples, mostly up to 15%. However, in horizons with muscovite as a dominant mineral, they prevail in HMF (Table 2). Chlorite is more abundant than biotite, often as a product of alteration of biotite, preserving its relict brown color. Exception with 68% of biotite is noticed in specific composition of HMF horizon of ZI-11. The reason could be the lack of grains of HMF in 0.09–0.16 mm fraction. Thus, after the analysis of 100 grains of 0.09–0.16 mm fraction, another set of 250 grains of 0.063–0.09 mm were additionally analyzed and added to the previous results. Specific composition of HMF of the ZI-11 horizon could result from the grain-size fractionation during transport and

Fig. 11. Laminated sediments in the Zmajevac section.

Fig. 12. Laminated sediments in the Erdut section.

Fig. 13. Muscovite-rich horizon Z-8 inhabited by insects. Red label is 20 cm long.

Fig. 14. Muscovite-rich horizon Z-1 inhabited by birds.

sedimentation of the material, or different source area of the horizon. The oldest horizons in the Zmajevac section (Z-38–Z-42) is enriched in biotite and chlorite and thus depleted in TMF (Table 2).

The most abundant transparent heavy minerals are resistant garnet grains (14–65%) followed by epidote (4–43%) and amphibole (4–40%) (Table 2, Figs. 7–10). Garnet grains are semi rounded, colorless to pink, corroded, and mostly presented by 26–44%. The epidote–zoisite group is presented with equidimensional, irregular, weathered grains. Epidote is usually yellow to greenish-yellow and shows weak pleochroism, while zoisite is colorless and with characteristic anomalous blue interference color, mostly presented by 10–25%. Amphiboles occur typically with 20–30%, represented by hornblende-type amphiboles, tremolite and, rarely, glaucophane. Grains are elongated sometimes without pronounced cleavage and pleochroism due to the presence of alteration products. Hornblende-type amphiboles of various colors (green – olive green, pale brown – brown, or dark greenish brown) are the most abundant amphiboles.

Less abundant pyroxenes, kyanite, staurolite, tourmaline, zircon, rutile and titanite occur regularly. This heavy mineral association is similar to the Danube flood plain sediments (Thamó-Bozsó and Kovács, 2007).

5. Discussion

Analysis of modal composition of loess showed significant differences in the composition of LMF (proportion of muscovite in the composition of LMF) (Table 2, Figs. 7–10), which indicates the different source area and the origin of the wind redeposited material. This does not exclude the possibility of the existence of erosional border between sediments from different deposition phases of loess, not visible during the field work in the commonly

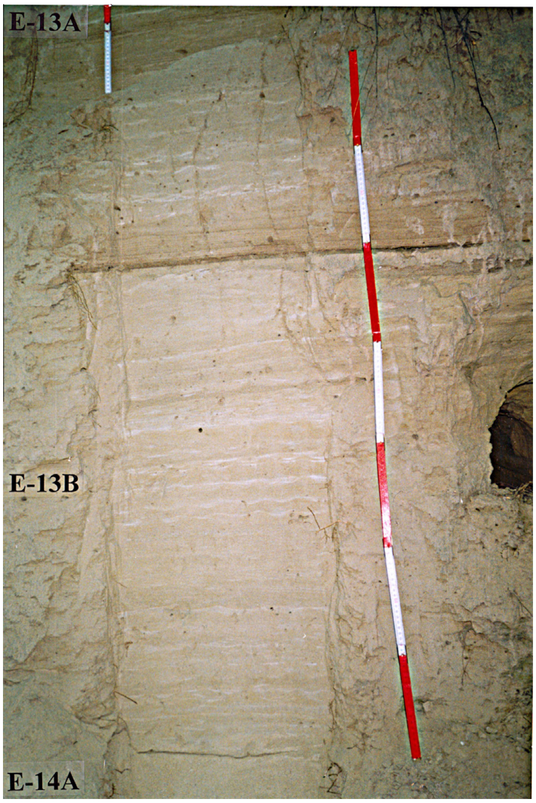

Fig. 15. Muscovite-rich horizon E-13B inhabited by mammals. Alteration of course and fine grained material in about 40 laminas. On the right side of the figure is entrance of burrow. Red label is 20 cm long.

massive homogeneous sediment. The source material for horizons rich in muscovite could be regional Tertiary sediments originated from muscovite-rich rocks of the Slavonian Mountains (Balen et al., 2006; Pamić et al., 2002) but also muscovite separated from secondary enriched Tertiary sediments that were redeposited by wind on this site. Larger amounts of chemically stable muscovite suggest the possibility of more cycles of repeated resedimentation, in this case resedimentation of Mesozoic and, particularly Neogene sedimentary rocks. Frechen et al. (2003) and Galović (2014) point out the importance of both Alpine and the local source areas for aeolian sediments in the Pannonian basin. Muscovite-rich sediment makes interbeds of decimeter to meter dimensions within the loess standard composition (Galović et al., 2009; Galović, 2014). If they were formed by resedimentation of the muscovite-rich sediments, laminated horizons will also show a very high percentage of this mineral (e.g. laminated sediments in the sections Zmajevac and Erdut, Figs. 8, 9, 11 and 12, Table 2).

Fig. 16. Contact of laminated horizon and underlying loess with ripple marks. Water energy was sufficiently powerful to transport large loess dolls sedimented with visible inclination.

All horizons rich in muscovite are characterized by recent in-drilling of organisms (insects (Fig. 13), birds (Fig. 14), mammals (Fig. 15)). The upper part of the Zmajevac section (Fig. 11) inhabited by insects and birds and it had been exposed only eight years before the field-work. Probably the high proportions of geochemically resistant mica, with a smaller proportion of clay minerals, contributed to airability of sediment and lack of moisture creating favorable life conditions. This in-drilling is significant since it facilitates the macroscopic field observation of such bands within seemingly homogenous loess. Namely, after digging out a half of meter of surface of section and thus removing that part of sediments in which insects are in-drilled, there is no longer possible to distinguish by macroscopic field methods the interbeds rich in muscovite from the upper and lower loess (E-6–E-7 and E-12A–E-12B). In addition, on the basis of observed in-drilling holes during the field work, it can be assumed that the dominant mineral in those horizons is muscovite. McLaren et al. (2014), based on the study of the European bee-eaters (Smalley et al., 2013), shows how loess does offer a remarkable combination of strength and liability to excavation which makes it excellent nesting ground. In the Zmajevac section bee-eaters are nested in the uppermost Z-1 horizon (Fig. 14), where insects (probably their food) are in-drilled in the Z-8 horizon (Fig. 13). Thus, casual connection between loess and inhabited organisms is rather comprehensive, since less than eight years period was long enough for creation of this biocenosis.

However, based on analyzed weathering coefficients, it cannot be concluded safely that minerals in the muscovite-rich horizons have been exposed to intensive weathering (Galović, 2014: Figs. 9–11). Another cause of muscovite enrichment could be its flaky shape which significantly enhanced the aeolian transport. Namely, there is a possibility that the wind force that caused muscovite-enrichment in sediments was too weak to transport larger quantities of quartz grains causing the separation between mica and granular minerals. Since the muscovite-rich layers have homogeneous composition down the profile, it can be concluded that there was no enrichment during, or after, deposition of aeolian sediment while the muscovite-rich material was homogenized before, or during, aeolian transport and then deposited as homogeneous sediment, mainly consisting of muscovite. Many publications present modal compositions of loess in Croatia, Hungary, Moravia in the Czech Republic and Serbia (Adamova et al., 2002; Bačani et al., 1999; Bronger, 1976, 2003; Durn, 2003; Pécsi-Donáth, 1985; Romić et al., 2014; Rubinić et al., 2015). They indicate a homogeneous and uniform composition of loess, dominated by quartz and in none authors found horizons with more than 50% muscovite. This is another evidence of a local source area. Domination of flaky minerals was observed in several horizons of some loess sections in Eastern Croatia (Banak et al., 2013; Wacha et al., 2013), which correlate to the Last Glacial period (Galović et al., 2009). Namely, due to the high mobility of flaky minerals (higher than those of the isometric or elongated ones), it is very likely that they were transported farther and from a more distal source (Thamó-Bozsó et al., 2014). On the other hand, Thamó-Bozsó et al. (2014) in Fig. 4 showed that NNW winds could supply the wider Transdanubian area, and hence also northern Croatia, with aeolian material of such a mineral composition. The chlorite- and/or biotite-rich heavy mineral associations of loess from South-Transdanubia are similar in their compositions to the recent fluvial sediments of the Danube and other Transdanubian rivers (Thamó-Bozsó et al., 2014) and could also be the source area for (re)sedimentation (Galović, 2014). Thus, beside the Danube, Drava and Sava River flood plains, part of the analyzed sediments could also originate from the nearby Slavonian Mountains, which are rich in granite (as a muscovite-bearing rock). This is supported by simulations of paleowind patterns in the Carpathian Basin during the Last Glacial Period as proposed by Újvári et al. (2010), showing WSW wind directions.

Fig. 17. Muscovite-rich horizon Z-1 inhabited by birds. Red label is 20 cm long.

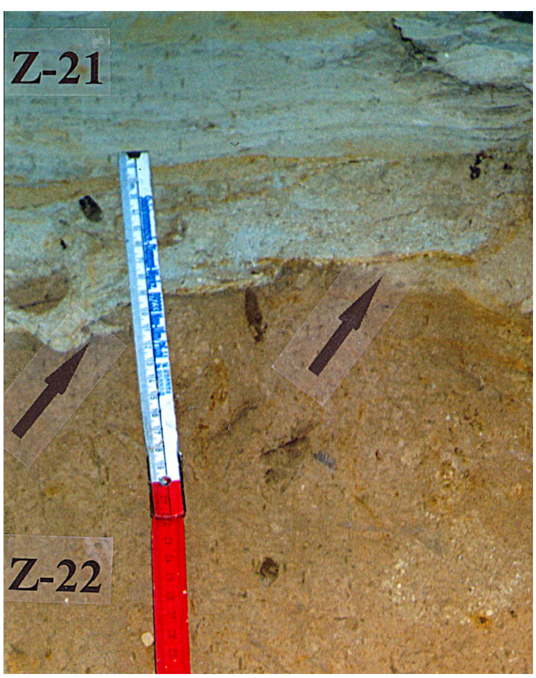

Fig. 18. Erosional border between laminated horizon Z-21 and paleosol horizon Z-22. Red label is 20 cm long.

In general, heavy mineral association is similar to the Danube flood plain sediments (Thamó-Bozsó and Kovács, 2007) and loess from Hungary (Thamó-Bozsó et al., 2014) but the southern edge of the Carpathian Basin was very likely influenced by the nearby Dinaride Ophiolite Zone (Rubinić et al., 2015). Garnet, amphibole and epidote-zoisite are dominant minerals within the THM composition of all samples (Table 2). This indicated the Danube floodplain region (Thamó-Bozsó and Kovács, 2007) and redeposited loess from Hungary (Thamó-Bozsó et al., 2014) to be the main source of the material. Since the Danube River originates from the same region as the Sava and the Drava Rivers (the Alpine region), their mineral composition resemble. The abundant pyroxenes in the Šarengrad section (Table 2), could originate from the Dinaride Ophiolite Zone in Bosnia (Pamić et al., 2002), being eroded by the Sava's southern tributaries. Šarengrad section is the southernmost among the analyzed sections and the closest to the Sava River floodplain and, thus, the most influenced by minerals from the Dinaride Ophiolite Zone in Bosnia. Buggle et al. (2008) geochemically characterized the loess/paleosol sections of Batajnica/Stari Slankamen (Serbia), Mircea Voda (Romania) and Stary Kaydaky (Ukraine) in order to identify the origin of south-eastern and Eastern European loess deposits. They concluded that the Danube catchment area is the most important for the Pleistocene delivery of the silt-sized alluvial sediments in the area. However, they also considered the Drava and Sava Rivers as the further important silt sources supplying glacio-fluvial sediments of the eastern Alps, with respect to the element composition and weathering products (Galović, 2014).

Laminated sediments of meter thicknesses (Fig. 15) occur within the analyzed sections. They are superimposed (with erosional border) on loess (Erdut (Figs. 12 and 16) and Šarengrad (Fig. 17)), or on paleosol (Zmajevac (Fig. 18)), and they are covered with loess (Erdut, Zmajevac), or paleosol (Šarengrad). Based on correlation of the dating results, they are not of the same age (Fig. 3). Modal and chemical compositions (Table 2) are unvarying and correspond to the loess/paleosol sequences (Galović, 2014; Galović et al., 2011). Thus, it can be concluded that the laminated sediments have been deposited in an aqueous medium. Grain size, modal, and chemical composition of those laminated sediments suggest that the laminas are composed of resedimented loess and pedogenetic carbonates. Thin parallel laminae indicate the tranquil conditions of sedimentation while the erosional border at the base of each cycle is indicate that the foot wall laminae were soft at the time of their reappearance on the new material (Fig. 19). The base of each cycle is the course-grained material with lag-sediment (pedorelicts of mm dimensions, detrital carbonate coatings, terrestrial gastropods shells, small fragments of carbonate concretions, or, in condition of sufficiently powerful

Fig. 19. Laminated horizon Z-21 with fine-grained material characterized by wavy and parallel lamination with streaming and parting lineation, or small angles of inclination. Red label is 20 cm long.

Fig. 20. Slumping of laminated sediment in the Erdut section. Water energy was sufficiently powerful to transport large loess dolls sedimented with visible inclination.

water energy, large loess dolls with visible inclination (Figs. 16 and 20). The grain size reduces upwards (fining upward cycles) but overall composition correlates to the loess/paleosol sections of drainage-basins (about 80% is silt). Course-grained material is darker brown due to the presence of terrigenous organic matter and has a parallel lamination, while fine-grained material is grayish with wavy and parallel lamination with streaming and parting lineation, or small angles of inclination (Figs. 15–19). If originated as a lake facies, laminae would contain macrofossils (e.g. root remains, charcoal or preserved gastropod shells) while in the case of marshy facies (anoxic facies), sediment would contain much more organic matter. Most likely, these laminated sediments are crevasse splay deposits, or local floodplain sediments. The large lowland rivers were meandering and forming natural river levees. During the warm period, large amounts of ice melted and significantly increased the water face and energy of waterways. Torrent streams eroded loess/paleosols draining the eroded material (sediment) toward morphologically lower parts of the relief. Rivers rupture the natural river levees and flooded into the surrounding plains. By distancing from the main flow, the energy of water and grain size of sediments have been reduced. It was reflected in small-ripple bedding (Figs. 16, 19 and 21). Each new seasonal warming caused a rise of water level in the river resulting with the occurrence of torrents, possibly with new flooding and erosion of the surface sediments (finest laminae – Fig. 19) of floodplains marking the onset of a new cycle of sedimentation. The sudden flows of water form the new erosional channels, which may, after lowering water level, be filled by sliding (slamps) with surrounding laminated sediments (Fig. 20) and sediments with ripple bedding (Fig. 21). Usually, the lower parts of laminated sediments contain thin parallel laminae with cycles approximately 1 mm thick (Fig. 17). Becoming more intense, the worming produced higher energy of water, which caused stronger floods and accumulation

Fig. 21. Moulds of ripple marks of small amplitude exposed in ceiling of basement in the Erdut section. Diameter of swallow's nest is approximately 20 cm.

of thicker laminae. Investigated sections are located close to meanders of the Drava and Danube Rivers, which is why those rivers or their tributaries can be assumed to penetrate their natural levees and flood, creating crevasse splay deposits, or local floodplain sediments. Since the Šarengrad section is 1 km east of the discovered, almost 10 m thick laminated sediment, and the section in Vukovar does not contain this type of sediment (Wacha and Frechen, 2011), it can be assumed that the shape of laminated sediments analyzed within this study area is in the form of elongated lens. Furthermore, it should be pointed out that warming periods are not represented just by paleosols, but also with laminated alluvial sediments.

6. Conclusions

(1) Beside the Danube, Drava and Sava River flood plains, part of the analyzed sediments also originates from regional Tertiary sediments originated from muscovite-rich rocks of the nearby Slavonian Mountains, which are rich in granite (as a muscovite-bearing rock), indicating the local influence.
(2) Enrichment of pyroxenes in the Šarengrad section points to the Dinaride Ophiolite Zone as its source of origin eroded by the Sava River southern tributaries. Šarengrad section is the southernmost among the analyzed sections, the closest to the Sava River floodplain and the southern edge of the Carpathian Basin. Thus, beside the Alpine region, the mineral composition is influenced by minerals from the Dinaride Ophiolite Zone in Bosnia.
(3) Sedimentological and mineralogical characteristics of the Pleistocene loess/paleosol sections in the Eastern Croatia show consistent sources area of aeolian sediments as geochemical archive of analyzed sections (Galović, 2014).
(4) Warming periods are not represented just by paleosols, but also with laminated alluvial sediments. During the warm period, large amounts of ice melted and significantly increased the water face and energy of waterways, powerful enough to transport large loess dolls. Unlike paleosols that present geochemically exchanged, but physically preserved sediment, in most cases alluvial sediments present physical erosion of underlying sediments (hiatus) followed by deposition of laminas.
(5) Recent settling of organisms is characteristic for all horizons with muscovite as a dominant mineral. High ratio of resistant platy mineral enabled airability and dryness of sediment insuring good living conditions. This in-drilling is important, because it enables clear identification of layers with specific mineral composition during the field investigation.
(6) Muscovite grains, finally transported by wind can successfully be distinguished from the ones transported by aquatic media, based on their edge and surface micro textures. The aeolian transported grains show less rounded edges with micro fractured mica plates. Its surface is blocky in appearance and often covered with impact marks, whereas the fluvial grains have nice rounded edges and smoother surface.
(7) Mohs scale number for quartz is 7, so its grains preserve abrasion marks of long transport. Furthermore, muscovite Mohs scale number is 2–2.5, thus leafs preserve abrasion marks of the last transport.

Acknowledgement

This work has been supported in part by Croatian Science Foundation under the project 4425 SAPIQ. I am very thankful to Dr. Hrvoje Posilović for mounting samples and scanning by SEM, for fruitful and incentive discussions and for review. I am also grateful to Dr. Zoran Peh for stimulating comments, constructive reviews and language editing. Very special thanks to anonymous reviewer for detailed and thoughtful reviews which significantly improved the manuscript.

References

Adamova, M., Havlíček, P., Šibrava, V., 2002. Mineralogy and geochemistry of loesses in Southern Moravia. Bull. Czech. Geol. Surv. 77 (1), 29–41.

Aitchison, J., 1986. The Statistical Analysis of Compositional Data. Chapman and Hall, London, New York.

Aitchison, J., 1997. The One-hour Corse in Compositional Data Analysis or Compositional Data Analysis. IAMG97, pp. 33.

Antoine, P., Rousseau, D.D., Fuchs, M., Hatté, C., Gauthier, C., Marković, S.B., Jovanović, M., Gaudenyi, T., Moine, O., Rossignol, J., 2009. High-resolution record of the last climatic cycle in the southern Carpathian Basin (Surduk, Vojvodina, Serbia). Quat. Int. 198, 19–36.

Bačani, A., Šparica, M., Velić, J., 1999. Quaternary deposits as the hydrogeological system of Eastern Slavonia. Geol. Croat. 52 (2), 141–152.

Balen, D., Horvath, P., Tomljenović, B., Finger, F., Humer, B., Pamić, J., Arkai, P., 2006. A record of pre-Variscan Barrovian regional metamorphism in the eastern part of the Slavonian Mountains (NE Croatia). Mineral. Petrol. 87, 143–162.

Banak, A., Mandić, O., Kovačić, M., Pavelić, D., 2012. Late Pleistocene climate history of the Baranja loess plateau – evidence from the Zmajevac loess–paleosol section (Northeastern Croatia). Geol. Croat. 65 (3), 411–422.

Banak, A., Pavelić, D., Kovačić, M., Mandić, O., 2013. Sedimentary characteristics and source of loess in Baranja (Eastern Croatia). Aeolian Res. 11, 129–139.

Bokhorst, M.P., Beets, C.J., Marković, S.B., Gerasimenko, N.P., Matviishina, Z.N., Frechen, M., 2009. Pedo-chemical climate proxies in late pleistocene Serbian–Ukranian loess sequences. Quat. Int. 198, 113–123.

Bronger, A., 1976. Zur quartären Klima-und Landschaftsentwicklung des Karpatenbeckens auf (palaeo)-pedologischer und bodengeographischer Grundlage. Kieler Geographische Schriften 45.

Bronger, A., 2003. Correlation of loess–paleosol sequences in East and Central Asia with SE Central Europe: towards a continental quaternary pedostratigraphy and paleoclimatic history. Quat. Int. 106 (107), 11–31.

Buggle, B., Glaser, B., Zöller, L., Hambach, U., Marković, S., Glaser, I., Gerasimenko, N., 2008. Geochemical characterization and origin of Southeastern and Eastern European loesses (Serbia, Romania, Ukraine). Quat. Sci. Rev. 27 (9-10), 1058–1075.

Buggle, B., Glaser, B., Hambach, U., Gerasimenko, N., Marković, S., 2011. An evaluation of geochemical weathering indices in loess–paleosol studies. Quat. Int. 240, 12–21.

CGS-Department for Geology, 2009. Geological Map of Republic of Croatia, M 1:300.000. Croatian Geological Survey, Department for Geology, Zagreb.

Durn, G., 2003. Terra rossa in the Mediterranean region: parent materials, composition and origin. Geol. Croat. 56 (1), 83–100.

Durn, G., Ottner, F., Slovenec, D., 1999. Mineralogical and geochemical indicators of the polygenetic nature of terra rossa in Istria. Geoderma 91 (1–2), 125–150.

Durn, G., Aljinović, D., Crnjaković, M., Lugović, B., 2007. Heavy and light mineral fractions indicate polygenesis of extensive terra rossa soils in Istria Croatia. In: Mange, M.A., Wright, D.T. (Eds.), Heavy Minerals in Use, Developments in Sedimentology, vol. 58. Elsevier, FAO, pp. 701–737, FAO, 2006. Guidelines for soil description, fourth ed. FAO, Rome.

Durn, G., Ćorić, R., Tadej, N., Barudžija, U., Rubinić, V., 2014. Bulk and clay mineral composition indicate origin of terra rossa soils in Western Herzegovina. Geol. Croat. 67 (3), 171–183.

Fitzsimmons, K.E., Marković, S.B., Hambach, U., 2012. Pleistocene environmental dynamics recorded in the loess of the middle and lower Danube basin. Quat. Sci. Rev. 41, 104–118.

Frechen, M., Oches, E.A., Kohfeld, K.E., 2003. Loess in Europe—mass accumulation rates during the Last Glacial Period. In: Derbyshire, E. (Ed.), Loess and the Dust Indicators and Records of Terrestrial and Marine Palaeoenvironments (DIRTMAP) database. Quat. Sci. Rev. 22, 1835–1857.

Frechen, M., Pécsi, M., 2004. Abony brickyard: IRSL and TL analysis of "Infusion Loess", vol. 4. Loess InForm, Budapest, pp. 63–70.

Galović, I., Mutić, R., 1984. Gornjopleistocenski sedimenti istočne Slavonije (Hrvatska). Rad JAZU 411, 299–356, Zagreb, (in Croatian).

Galović, L., 2014. Geochemical archive in the three loess/paleosol sections in the Eastern Croatia: Zmajevac I, Zmajevac and Erdut. Aeolian Res. 15, 113–132.

Galović, L., Frechen, M., Halamić, J., Durn, G., Romić, M., 2009. Loess chronostratigraphy in Eastern Croatia – a luminescence dating approach. Quat. Int. 198 (1–2), 85–97.

Galović, L., Frechen, M., Peh, Z., Durn, G., Halamić, J., 2011. Loess/palaeosol section in Šarengrad, Croatia – a qualitative discussion on the correlation of the geochemical and magnetic susceptibility data. Quat. Int. 240 (1–2), 22–34.

Gorjanović-Kramberger, D., 1912. Iz prapornih predjela Slavonije. Vijesti Geol. Povjerensztva 2, 28–30, Zagreb, (in Croatian).

Gorjanović-Kramberger, D., 1914. Iz prapornih predjela Slavonije. Vijesti Geol. Povjerenszva 3/4, 21–26, Zagreb, (in Croatian).

Haase, D., Fink, J., Haase, G., Ruske, R., Pecsi, M., Richter, H., Altermann, M., Jager, K. D., 2007. Loess in Europe – its spatial distribution based on a European Loess Map, scale 1:2.500.000. Quat. Sci. Rev. 26, 1301–1312.

Hupuczi, J., Molnár, D., Galović, L., Sümegi, P., 2010. Preliminary malacological investigation of the loess profile at Šarengrad, Croatia. Cent. Eur. J. Geosci. 2 (1), 57–63.

Krinsley, D.H., Donahue, J., 1968. Environmental interpretation of sand grain surface textures by the scanning electron microscope. Trans. N.Y. Acad. Sci. Ser. 31, 457–477.

Mahaney, W.C., Stewart, A., Kalm, V., 2001. Quantification of SEM microtextures useful in sedimentary environmental discrimination. Boreas 30, 165–171.

Marković, S.B., Hambach, U., Catto, N., Jovanović, M., Buggle, B., Machalett, B., Zöller, L., Glaser, B., Frechen, M., 2009. Middle and late Pleistocene loess sequences at Batajnica, Vojvodina, Serbia. Quat. Int. 198, 255–266.

Marković, S.B., Hambach, U., Stevens, T., Kukla, G.J., Heller, F., McCoy, W.D., Oches, E. A., Buggle, B., Zöller, L., 2011. The last million years recorded at the Stari Slankamen (Northern Serbia) loess-palaeosol sequence: revised chronostratigraphy and long-term environmental trends. Quat. Sci. Rev. 30, 1142–1154.

Marković, S.B., Hambach, U., Stevens, T., Jovanović, M., O'Hara-Dhand, K., Basarin, B., Lu, H., Smalley, I., Buggle, B., Zech, M., Svirčev, Z., Sümegi, P., Milojković, N., Zöller, L., 2012. Loess in the Vojvodina region (Northern Serbia): an essential link between European and Asian Pleistocene environments. Neth. J. Geosci. 91 (1–2), 173–188.

Mazzullo, J., Ritter, C., 1991. Influence of sediment source on the shapes and surface textures of glacial quartz sand grains. Geology 19, 384–388.

McLaren, S., Svircev, Z., O'Hara-Dhand, K., Heneberg, P., Smalley, I., 2014. Loess and bee-eaters II: the 'loess' of North Africa and the nesting behaviour of the Northern carmine bee-eater (Merops nubicus Gmelin 1788). Quat. Int. 334 (335), 112–118.

Molnár, D., Hupuczi, J., Galović, L., Sümegi, P., 2010. Preliminary malacological investigation on the loess profile at Zmajevac, Croatia. Cent. Eur. J. Geosci. 2 (1), 52–56.

Munsell Soil Color Charts, 2000. Munsell Soil Color Charts. Macbeth Division of Kollmorgem Instruments Corporation, New Windsor.

Mutić, R., 1990. Korelacija kvartara istočne Slavonije na osnovi podataka mineraloško-petrografskih analiza (Istočna Hrvatska, Jugoslavija) – Dio II: Lesni ravnjak. Acta Geol. 20 (2), 29–80, Zagreb, (in Croatian).

Pamić, J., Pikija, M., 1987. Badenian andesites and pyroclastics from Baranja in northern Croatia (Yugoslavia). Acta Geol. Hung. 30 (1–2), 111–132.

Pamić, J., Tomljenović, B., Balen, D., 2002. Geodynamic and petrogenetic evolution of Alpine ophiolites from the Central and NW Dinarides: an overview. Lithos 65, 113–142.

Pécsi-Donáth, É., 1985. On the mineralogical and petrological properties of the younger loess in Hungary. In: Pécsi, M. (Ed.), Loess and the Quaternary. Akadémiai Kiadó, Budapest, pp. 93–104.

Poje, M., 1985. Praporne naslage "vukovarskog profila" i njihova stratigrafska pripadnost. Geol. Vjesn. 38, 45–66 (in Croatian).

Poje, M., 1986. Ekološke promjene na vukovarskom prapornom ravnjaku proteklih cca 500.000 godina. Geol. Vjesn. 39, 19–42 (in Croatian).

Romić, M., Bragato, G., Zovko, M., Romić, D., Mosetti, D., Galović, L., Bakić, H., 2014. The characteristics of soils developed from coastal paleosand (Korčula Island, Croatia). Catena 113, 281–291.

Rubinić, V., Durn, G., Husnjak, S., Tadej, N., 2014. Composition, properties and formation of Pseudogley on loess along a precipitation gradient in the Pannonian region of Croatia. Catena 113, 138–149.

Rubinić, V., Galović, L., Husnjak, S., Durn, G., 2015. Climate vs. parent material – which is the key of Pseudogley diversity in Croatia? Geoderma 241 (242), 250–261.

Rukavina, D., 1983. O stratigrafiji gornjeg pleistocena s osvrtom na topla razdoblja i njihov odraz u naslagama na području Jugoslavije. Rad. JAZU 19, 199–221, Zagreb, (in Croatian).

Singhvi, A.K., Bronger, A., Sauer, W., Pant, R.K., 1989. Thermoluminescence dating of loess-paleosol sequences in the Carpathian basin (East-Central Europe): a suggestion for a revised chronology. Chem. Geol. (Isotope Science Section) 73, 307–317.

Smalley, I.J., O'Hara-Dhand, K., McLaren, S., Svircev, Z., Nugent, H., 2013. Loess and bee-eaters I: ground properties affecting the nesting behaviour of European bee-eaters (Merops apiaster L. 1758) in loess deposits. Quat. Int. 296, 220–226.

Thamó-Bozsó, E., Kovács, L., 2007. Evolution of quaternary to modern fluvial network in the Mid-Hungarian plain, indicated by heavy mineral distributions and statistical analysis of heavy mineral data. In: Heavy Minerals in Use. In: Mange, M., Wright, D. (Eds.), . Developments in Sedimentology, vol. 58. Elsevier, Amsterdam, pp. 491–514.

Thamó-Bozsó, E., Kovács, L.O., Magyari, Á., Marsi, I., 2014. Tracing the origin of loess in Hungary with the help of heavy mineral composition data. Quat. Int. 319, 11–21.

Újvári, G., Kovács, J., Varga, G., Raucsik, B., Marković, S.B., 2010. Dust flux estimates for the last glacial period in East Central Europe based on terrestrial records of loess deposits: a review. Quat. Sci. Rev. 29, 3157–3166.

Újvári, G., Varga, A., Raucsik, B., Kovács, J., 2014. The Paks loess-paleosol sequence: a record of chemical weathering and provenance for the last 800 ka in the mid-Carpathian basin. Quat. Int. 319, 22–37.

Ujházy, K., Gábris, G., Frechen, M., 2003. Ages and periods of sand movement in Hungary determined through luminescence measurements. Quat. Int. 111, 91–100.

Wacha, L., Frechen, M., 2011. The chronology of the "Gorjanović loess section" in Vukovar. Croat. Quat. Int. 240, 87–99.

Wacha, L., Galović, L., Koloszár, L., Magyari, Á., Chikán, G., Marsi, I., 2013. The chronology of the Šarengrad II loess–palaeosol section (Eastern Croatia). Geol. Croat. 66 (3), 191–203.